

## Solvatofluorochromism

# Symmetry Breaking in Pyrrolo[3,2-*b*]pyrroles: Synthesis, Solvatofluorochromism and Two-photon Absorption

Łukasz G. Łukasiewicz,<sup>[a]</sup> Hye Gun Ryu,<sup>[a, b]</sup> Alexander Mikhaylov,<sup>[c]</sup> Cloé Azarias,<sup>[d]</sup> Marzena Banasiewicz,<sup>[e]</sup> Bolesław Kozankiewicz,<sup>\*,[e]</sup> Kyo Han Ahn,<sup>\*,[b]</sup> Denis Jacquemin,<sup>\*,[d, f]</sup> Aleksander Rebane,<sup>\*,[c, g]</sup> and Daniel T. Gryko<sup>\*,[a]</sup>

**Abstract:** Five centrosymmetric and one dipolar pyrrolo[3,2-*b*]pyrroles, possessing either two or one strongly electron-withdrawing nitro group have been synthesized in a straightforward manner from simple building blocks. For the symmetric compounds, the nitroaryl groups induced spontaneous breaking of inversion symmetry in the excited state, thereby leading to large solvatofluorochromism. To study the origin of this effect, the series employed peripheral structural motifs that control the degree of conjugation via altering of dihedral angle between the 4-nitrophenyl moiety and the electron-rich core. We observed that for compounds with a larger dihedral angle, the fluorescence quantum yield decreased quickly when exposed to even moderately polar solvents. Reducing the dihedral angle (i.e., placing the nitrobenzene moiety in the same plane as the rest of the molecule) moderated the dependence on solvent polarity so that the dye exhibited significant emission, even in THF. To investigate at what stage the symmetry breaking occurs, we mea-

sured two-photon absorption (2PA) spectra and 2PA cross-sections ( $\sigma_{2PA}$ ) for all six compounds. The 2PA transition profile of the dipolar pyrrolo[3,2-*b*]pyrrole, followed the corresponding one-photon absorption (1PA) spectrum, which provided an estimate of the change of the permanent electric dipole upon transition,  $\approx 18$  D. The nominally symmetric compounds displayed an allowed 2PA transition in the wavelength range of 700–900 nm. The expansion via a triple bond resulted in the largest peak value,  $\sigma_{2PA} = 770$  GM, whereas altering the dihedral angle had no effect other than reducing the peak value two- or even three-fold. In the  $S_0 \rightarrow S_1$  transition region, the symmetric structures also showed a partial overlap between 2PA and 1PA transitions in the long-wavelength wing of the band, from which a tentative, relatively small dipole moment change, 2–7 D, was deduced, thus suggesting that some small symmetry breaking may be possible in the ground state, even before major symmetry breaking occurs in the excited state.

## Introduction

Various two-photon absorbing organic chromophores have been developed over the last few decades.<sup>[1]</sup> Rationally designed two-photon absorbing materials are widely used in

multiphoton microscopy,<sup>[2]</sup> localized release of bio-active species,<sup>[3]</sup> optical power limiting,<sup>[4]</sup> 3D data storage<sup>[5]</sup> and 3D microfabrication.<sup>[6]</sup> Among various scaffolds, quadrupolar architectures<sup>[7,8]</sup> are often preferred as they exhibit larger two-photon absorption cross-sections than dipolar ones<sup>[9]</sup> and at

[a] Ł. G. Łukasiewicz, H. G. Ryu, Prof. D. T. Gryko  
Institute of Organic Chemistry  
Polish Academy of Sciences  
Kasprzaka 44–52, 01-224 Warsaw (Poland)  
E-mail: dtgryko@icho.edu.pl

[b] H. G. Ryu, Prof. K. H. Ahn  
Department of Chemistry  
POSTECH  
77 Cheongam-Ro, Nam-Gu, Pohang, Gyeongbuk 37673 (Korea)  
E-mail: ahn@postech.ac.kr


[c] A. Mikhaylov, Prof. A. Rebane  
Department of Physics  
Montana State University  
Bozeman, MT 59717 (USA)  
E-mail: arebane@montana.edu

[d] C. Azarias, Prof. D. Jacquemin  
CEISAM laboratory—UMR 6230  
University of Nantes  
2, rue de la Houssinière, 44322 Nantes (France)  
E-mail: Denis.Jacquemin@univ-nantes.fr

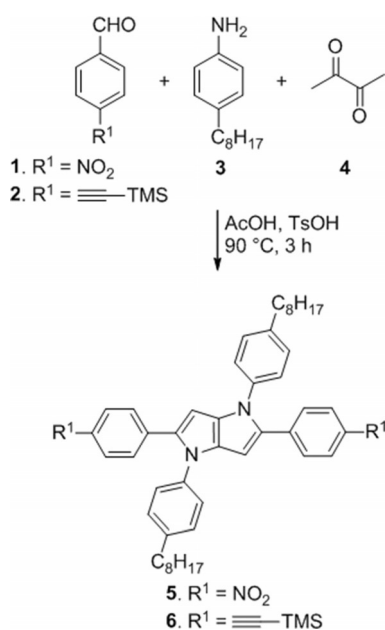
[e] Dr. M. Banasiewicz, Prof. B. Kozankiewicz  
Institute of Physics PAS  
Al. Lotników 32/46, 02-668 Warsaw (Poland)  
E-mail: kozank@ifpan.edu.pl

[f] Prof. D. Jacquemin  
Institut Universitaire de France  
1, rue Descartes, 75231 Paris Cedex 05 (France)

[g] Prof. A. Rebane  
National Institute of Chemical Physics and Biophysics  
Akadeemia tee 23, 12618 Tallinn (Estonia)

 Supporting information and the ORCID identification number(s) for the author(s) of this article can be found under <https://doi.org/10.1002/asia.201700159>.

the same time they possess smaller size than octupolar chromophores.<sup>[10]</sup> These quadrupolar, centrosymmetric molecules often do not display either solvatochromism or solvatofluorochromism. Notable exceptions have been pointed out by Terenziani and co-workers<sup>[11]</sup> and recently this phenomenon, i.e., symmetry breaking in the excited state has been intensively studied in various laboratories.<sup>[12]</sup> In this context, symmetry breaking in quadrupolar, centrosymmetric pyrrolo[3,2-*b*]pyrroles became the focus of our interest,<sup>[13]</sup> especially after we have discovered that the 2,5-bis(4-nitrophenyl)-1,4-bis(4-octylphenyl)-1,4-dihydropyrrolo[3,2-*b*]pyrrole (**5**, see Scheme 1) displayed very strong solvatofluorochromism. Its emission in cyclohexane was extremely strong while emission in moderately polar solvents such as CH<sub>2</sub>Cl<sub>2</sub> or THF was bathochromically shifted by 100 nm, with a fluorescence quantum yield ( $\Phi_f$ ) < 0.03.<sup>[14]</sup>



Scheme 1. Synthesis of compounds **5** and **6**.

This interesting discovery prompted us to perform an in-depth investigation of the influence of size of the  $\pi$ -system and the degree of conjugation (by changing the dihedral angle between heterocyclic core and nitrobenzene subunit) on the linear and non-linear optical properties of pyrrolo[3,2-*b*]pyrroles possessing 4-nitrophenyl substituents.

Until recently, strongly coupled dyes linked by double or triple bonds were prevailing in the literature;<sup>[15]</sup> however, weakly coupled chromophores containing biaryl linkages have drawn greater attention in last decade.<sup>[16]</sup> The critical advantage of the pyrrolo[3,2-*b*]pyrrole core in this regard is that it is the most electron-rich heterocycle among aromatic two-ring systems, in principle offering access to reasonable values of two-photon absorption cross-sections without the need to strongly couple the chromophores. Consequently, through modulation of the planarization and polarization, such dyes can at the same time respond to changes in the viscosity and possess strong two-photon response.

Aiming to better understand the relation between solvatofluorochromism and conformational motions (or lack thereof), we thus conceived a series of structures based on dye **5** as a core, where various moieties were chemically threaded or linked in different modes. Our aim was to impose various degrees of constraint to impede the symmetry breaking of the molecule in the excited state, thereby modulating photoluminescence.

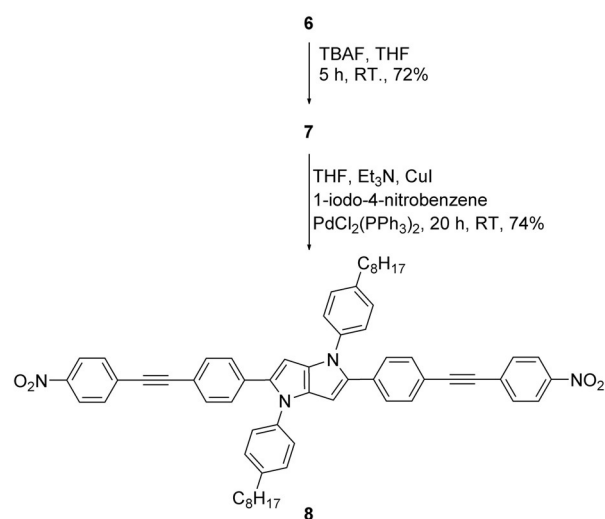
## Results and Discussion

### Design and synthesis

Prior research on tetraaryl-pyrrolo[3,2-*b*]pyrroles<sup>[13,14,17–20]</sup> has indicated that derivatives containing nitrophenyl substituents display especially pronounced solvatofluorochromism effects. Therefore we decided to focus exclusively on compounds possessing this strongly electron-withdrawing group. Maintaining pyrrolo[3,2-*b*]pyrrole as the central electron-rich unit and the 4-nitrophenyl group as the key moiety, we resolved to modulate the dihedral angle between these subunits by fusion of the rings or by adding substituents. 4-*n*-Octylaniline has been used to prepare all final products to ensure suitable solubility in organic solvents, so that the full set of spectroscopic analyses could be obtained. Foremost, however, we resolved to expand the  $\pi$ -system through insertion of two additional arylethynyl units between the core and the 4-nitrophenyl substituents. The synthesis of the required tetraaryl-pyrrolo[3,2-*b*]pyrrole **6** was conducted by following an established procedure (Scheme 1).<sup>[17–19]</sup>

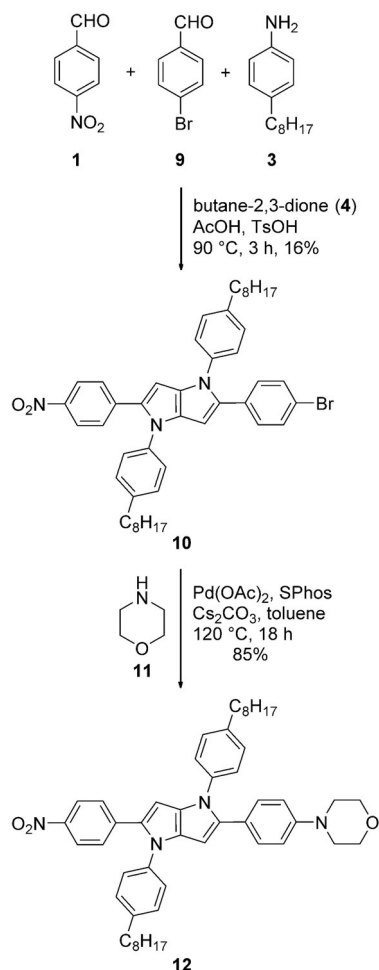
Subsequently, the smooth cleavage of the TMS group followed by Sonogashira reaction with 1-nitro-4-iodobenzene was performed, and compound **8** was obtained with satisfying yield of 74% (Scheme 2).

In the context of the present study, it was of interest to contrast centrosymmetric pyrrolo[3,2-*b*]pyrroles with the behavior of a dipolar analog possessing only one nitro group. The strong interaction between the electron-donating and elec-



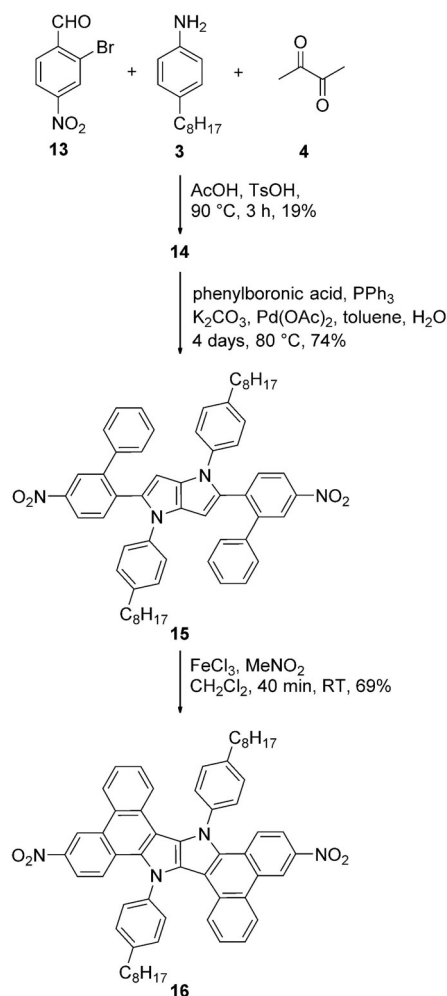
Scheme 2. Synthesis of compound **8**.

tron-withdrawing groups located at the ends of the pyrrolo[3,2-*b*]pyrrole has already been examined.<sup>[20]</sup> The synthesis of such nonsymmetric pyrrolo[3,2-*b*]pyrroles requires the presence of two different aldehydes in the initial condensation. The mixed-condensation using 4-bromobenzaldehyde and 4-nitrobenzaldehyde afforded dye **10**, containing one bromo functionality, in 16% yield. Subsequently, dye **10** was used in the Buchwald–Hartwig amination under the previously reported conditions<sup>[21]</sup> to give dipolar dye **12** (Scheme 3).



Scheme 3. Synthesis of compound **12**.

The dihedral angles between the phenyl groups located at positions 2 and 5 and the core of the molecule were about 35 degrees (see also modeling studies below)<sup>[14]</sup> which enabled electronic communication, but interaction of peripheral electron-accepting moieties with the electron-rich core would be stronger if both moieties were located within the same plane. To achieve this goal, we fused the benzene rings located at positions 2 and 5 with the core at positions 3 and 6. Aldehyde **13**, prepared as previously reported,<sup>[22]</sup> was subsequently transformed into pyrrolo[3,2-*b*]pyrrole **14**, containing two bromine atoms that enabled us to perform Suzuki coupling leading to dye **15** (Scheme 4).



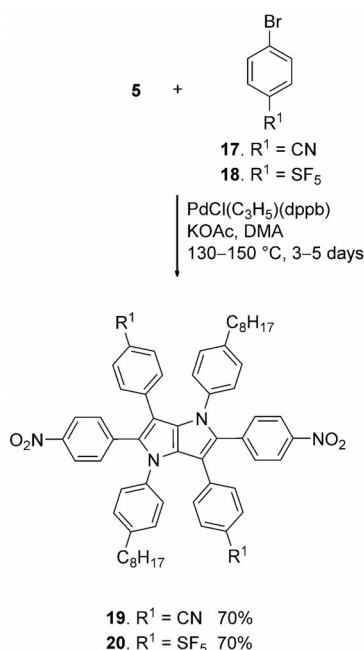
Scheme 4. Synthesis of compound **16**.

In the final step, an oxidative aromatic coupling was performed under previously described conditions<sup>[23]</sup> ( $\text{FeCl}_3$ ,  $\text{MeNO}_2$ ,  $\text{CH}_2\text{Cl}_2$ ) which led to the formation of compound **16** with a yield of 69% (Scheme 4).

Direct arylation is a particularly promising method of synthesizing functional dyes possessing biaryl linkages.<sup>[24]</sup> We have previously shown that this reaction is appropriate for pyrrolo[3,2-*b*]pyrroles,<sup>[19]</sup> if conditions developed by Doucet and co-workers are applied.<sup>[25]</sup> The arylation of model dye **5** with aryl bromides **17** and **18** possessing various electron-withdrawing groups was carried out (Scheme 5). The reactions proceeded with satisfying yield of 70% leading to hexaaryl-pyrrolo[3,2-*b*]pyrroles **19** and **20**.

### Linear absorption and emission properties

Figure 1 shows the absorption and fluorescence emission spectra of **8**, **12** and **16** in cyclohexane. The absorption maxima corresponded with of  $S_0 \rightarrow S_1$  transition occurs in the 400–500 nm range, whereas the fluorescence peak is shifted to longer wavelengths. Table 1 and Figures 2–4 summarize the linear absorption peak wavelengths, extinction coefficients,



Scheme 5. Synthesis of compounds 19 and 20.

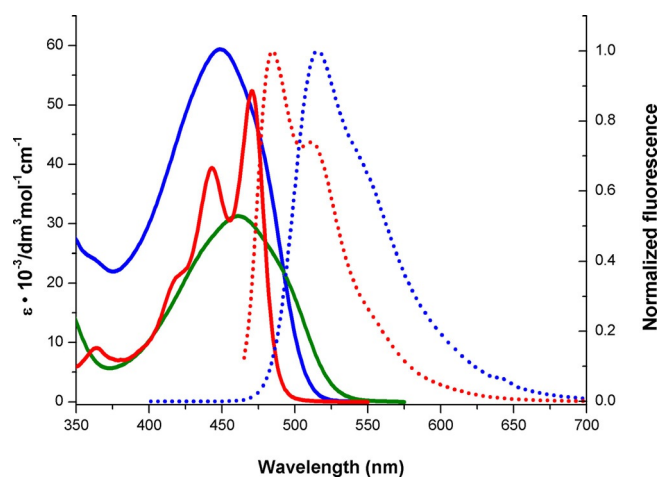


Figure 1. Absorption (solid) and emission (dotted) spectra of compounds 8 (blue), 12 (green), 16 (red) in cyclohexane.

and emission peak wavelengths of all six compounds obtained in a series of solvents of increasing polarity (cyclohexane, toluene, dichloromethane, THF and acetonitrile). When comparing the optical properties of dye 8 to model compound 5, the first surprising observation was the lack of a bathochromic shift of absorption (Table 1). We expected such a shift because in the previous study involving pyrrolo[3,2-*b*]pyrroles possessing carbon-carbon triple bonds<sup>[18]</sup> the comparison of two compounds possessing CN groups revealed that two arylethynyl units contributed to an about 20 nm shift of absorption in CH<sub>2</sub>Cl<sub>2</sub>. The emission for compound 8 was, however, bathochromically shifted in cyclohexane from 496 nm to 515 nm, and an even larger shift was observed in toluene. The heterocycle 8 differed from its previously studied, non-expanded

Table 1. Optical properties of dyes 5, 8, 12, 15, 16, 19 and 20.						
Compd	Solvent	$\lambda_{\text{abs}}$ [nm]	$\epsilon$ [M <sup>-1</sup> cm <sup>-1</sup> ]	$\lambda_{\text{em}}$ [nm]	$\Delta S$ [cm <sup>-1</sup> ]	$\Phi_{\text{fl}}$
5 <sup>[a]</sup>	C <sub>6</sub> H <sub>12</sub>	447, 469	48 000	496, 525	1200	0.96
	Toluene	465	42 000	552, 569	3400	0.70
	THF	471	44 000	610	4800	0.03
	CH <sub>2</sub> Cl <sub>2</sub>	477	41 000	nd	nd	nd
	CH <sub>3</sub> CN	467	40 000	nd	nd	nd
8	C <sub>6</sub> H <sub>12</sub>	449	59 400	515	3700	0.25
	Toluene	453	49 600	585	5000	0.03
	THF	450	53 900	nd	nd	0.00
	CH <sub>2</sub> Cl <sub>2</sub>	451	50 500	nd	nd	nd
	CH <sub>3</sub> CN	440	46 500	nd	nd	nd
12	C <sub>6</sub> H <sub>12</sub>	461	31 300	nd	nd	nd
	Toluene	473	27 200	nd	nd	nd
	THF	477	27 300	nd	nd	nd
	CH <sub>2</sub> Cl <sub>2</sub>	480	24 700	nd	nd	nd
	CH <sub>3</sub> CN	468	25 300	nd	nd	nd
15	C <sub>6</sub> H <sub>12</sub>	449	26 400	512	2700	0.59
	Toluene	461	26 700	566	4000	0.07
	THF	466	25 400	nd	nd	nd
	CH <sub>2</sub> Cl <sub>2</sub>	472	24 400	nd	nd	nd
	CH <sub>3</sub> CN	462	23 900	nd	nd	nd
16	C <sub>6</sub> H <sub>12</sub>	473	52 300	484	500	0.80
	Toluene	480	49 800	518	1500	0.72
	THF	477	50 400	547	2700	0.54
	CH <sub>2</sub> Cl <sub>2</sub>	483	49 200	636	5000	0.06
	CH <sub>3</sub> CN	479	13 000	661	5200	0.01
19	C <sub>6</sub> H <sub>12</sub>	432	32 900	476	2100	0.7
	Toluene	444	24 000	534	3800	0.25
	THF	449	27 100	600	5600	0.01
	CH <sub>2</sub> Cl <sub>2</sub>	460	26 600	nd	nd	0.00
	CH <sub>3</sub> CN	450	24 600	nd	nd	nd
20	C <sub>6</sub> H <sub>12</sub>	433	31 000	476, 503	2100	0.32
	Toluene	443	27 300	535	3900	0.13
	THF	447	26 800	nd	nd	nd
	CH <sub>2</sub> Cl <sub>2</sub>	459	26 900	nd	nd	nd
	CH <sub>3</sub> CN	448	24 300	nd	nd	nd

[a] Data taken from ref. [10].

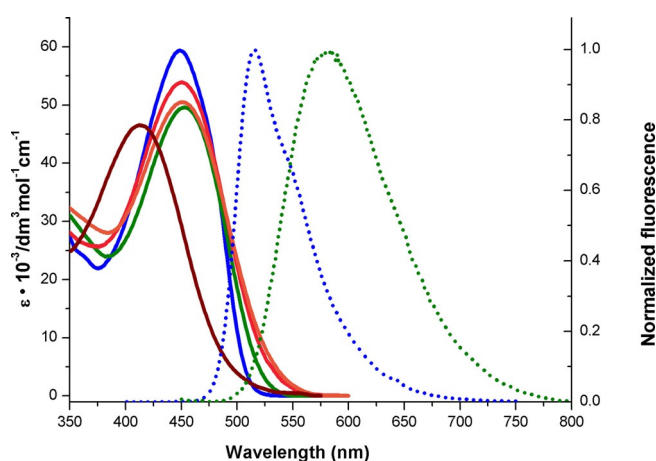
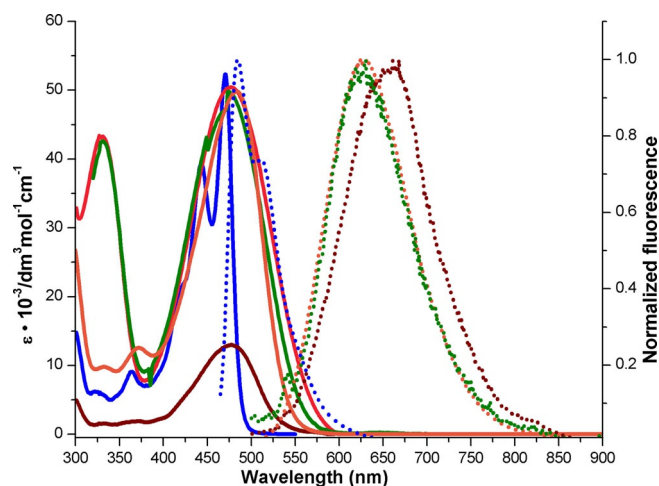


Figure 2. Absorption (solid) and emission (dotted) spectra of compound 8. Blue—cyclohexane, green—toluene, orange—dichloromethane, pink—THF, maroon—acetonitrile.

analog 5 by having a lower fluorescence quantum yield ( $\Phi_{\text{fl}}$ ) – in cyclohexane (25 % vs. 96 %).

When compared to its analog possessing two 4-cyanophenylethynyl substituents<sup>[18]</sup> or 4-formylphenylethynyl substitu-



**Figure 3.** Absorption (solid) and emission (dotted) spectra of compound **16**. Blue—cyclohexane, green—toluene, orange—dichloromethane, pink—THF, maroon—acetonitrile.

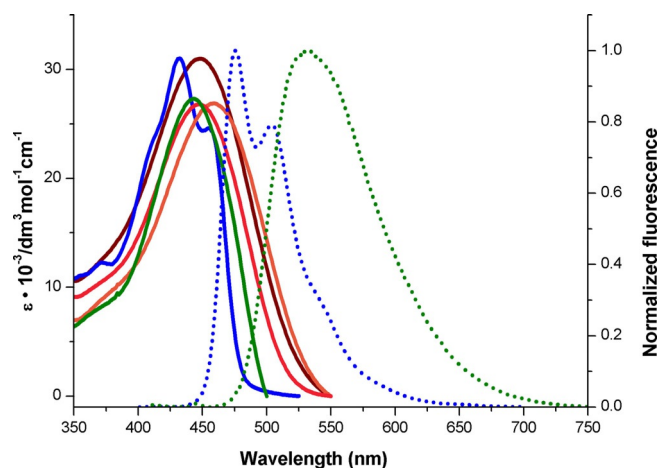


**Figure 4.** Absorption (solid) and emission (dotted) spectra of compound **19**. Blue—cyclohexane, green—toluene, orange—dichloromethane, pink—THF, maroon—acetonitrile.

ents, the absorption of dye **8** was shifted bathochromically, as expected, as a result of the presence of stronger electron-withdrawing groups. The emission could not be directly compared as the fluorescence of dye **8** was undetectable in  $\text{CH}_2\text{Cl}_2$ .

The dye **12** differs from the previously studied dipolar pyrrolo[3,2-*b*]pyrrole by having an  $\text{NO}_2$  end group instead of the CN group,<sup>[20]</sup> and this increased electron-withdrawing strength is manifested as the largest bathochromic shift, varying from 62 nm to 82 nm. Unfortunately, compound **12** did not exhibit fluorescence in any of the tested solvents.

Pyrrolo[3,2-*b*]pyrrole **15**, due to the presence of two sterically encumbering phenyl substituents, should have the largest dihedral angle between the heterocyclic core and the 4-nitrophenyl units. Absorption of this compound was, however, not shifted hypsochromically versus that of dye **5** (Table 1). Even its emission in cyclohexane was bathochromically shifted (from 496 nm to 512 nm). This effect clearly indicated that the additional benzene rings contributed to the  $\pi$ -expansion of the

conjugated system and that in the excited state the geometry was significantly more planar. Fluorescence quantum yields were observed in solvents of low polarity only, that is cyclohexane (0.59) and toluene (0.07), whereas in solvents of higher polarity (THF,  $\text{CH}_2\text{Cl}_2$  and acetonitrile), fluorescence was below our detection limit.

According to our expectations, fusion of the system, i.e., **15**→**16**, led to a very significant shift of absorption from 449 nm to 473 nm in cyclohexane. At the same time, emission in non-polar solvents was shifted hypsochromically. This effect had previously been observed for the analogous pyrrolo[3,2-*b*]pyrroles series. It was attributed to the disrupted conjugation of the *N*-aryl substituents after fusion at positions 3 and 6, as supported by an X-ray structures revealing that the dihedral angle was close to  $90^\circ$ .<sup>[23]</sup> In terms of solvatofluorochromism, compound **16** shared some common features with model compound **5**. It possessed a very high fluorescence quantum yield in cyclohexane, which decreased rapidly in the presence of polar solvents. The key difference is that the decrease in fluorescence quantum yield of compound **16** was slower and that fluorescence, regardless of the solvent, was hypsochromically shifted versus compound **5** (Table 1).

The comparison of the hexaaryl-pyrrolo[3,2-*b*]pyrroles **19** and **20** with model dye **5** revealed that they possess slightly hypsochromically shifted absorption ( $\approx 20$  nm in toluene) and emission ( $\approx 20$  nm in cyclohexane,  $\approx 5$  nm in toluene). Again, the higher dihedral angle in hexaaryl-pyrrolo[3,2-*b*]pyrroles was responsible for this effect. In the case of dye **19** possessing cyano groups, solvatofluorochromism was strong—emission maxima shifted hypsochromically while the fluorescence quantum yield decreased from 0.7 in cyclohexane to 0.01 in THF. Dye **20** possessing two  $\text{SF}_5$  groups displayed much weaker fluorescence, which resembled previously obtained hexaaryl-pyrrolo[3,2-*b*]pyrroles possessing  $\text{SF}_5$  groups.<sup>[19]</sup>

Fluorescence in the solid state has been measured as well (Figure 5 and Supporting Information). It was found that all studied pyrrolo[3,2-*b*]pyrroles including dye **12**, which does not fluoresce in solution, display emission in the crystalline state. The emission maxima were strongly bathochromically

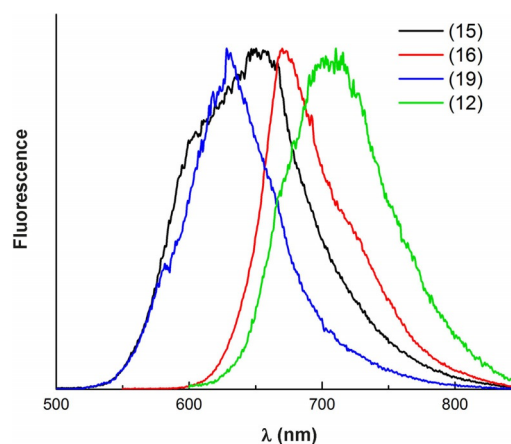


**Figure 5.** Emission of pyrrolo[3,2-*b*]pyrroles **12**, **15**, **16** and **19** in the solid state.

shifted compared to solution studies ( $\approx 100\text{--}150\text{ nm}$ ). The emission maximum of the dipolar dye **12** was at lower energy than that of its quadrupolar analogs.

### Two-photon absorption (2PA)

Femtosecond 2PA spectra were measured in the excitation wavelength range of  $\lambda_{2PA} = 600\text{--}1050\text{ nm}$  by using two-photon excited fluorescence (2PEF) and nonlinear transmission (NLT) methods (see the Experimental Section). The quadratic dependence of the 2PEF signal on the energy of the incident laser pulses was confirmed (for the 2PEF method) with an accuracy of  $2.00 \pm 0.05$  within the above-named wavelength range. At wavelengths  $\lambda_{2PA} < 600\text{ nm}$ , there was an increasing contribution of the accompanying one-photon excitation due to partial overlap between the laser spectrum and the  $S_0 \rightarrow S_1$  absorption band, which resulted in a decline of the power exponent from the strict quadratic dependence. Figure 6 shows the 2PA spectra of the six compounds studied in cyclohexane solution. For compounds **8**, **15**, **16**, **19** and **20**, i.e., for the five systems showing strong fluorescence emission ( $\Phi_f > 0.25$ ), the 2PEF excitation method was used, whereas for **12**, which lacked any measurable fluorescence signal, we used the NLT method. For verification purposes, both methods were applied for **8** and **20**. Linear absorption spectra in cyclohexane are shown for comparison. Peak  $\sigma_{2PA}$  values along with corresponding wavelengths are collected in Table 2.

For compounds **8**, **15**, **16**, **19**, and **20**, the maximum 2PA occurs around 790–820 nm (i.e., at a transition energy well above the one photon  $S_0 \rightarrow S_1$  transition peak). This result is consistent with the predominant behavior displayed by chromophores with nominally centrosymmetric or nearly centrosymmetric structures, including a previously reported series of peripherally substituted pyrrolo[3,2-*b*]pyrrole derivatives.<sup>[14]</sup> The maximum  $\sigma_{2PA}$  value (determined by the 2PEF method) is

Compound	Maximum $\sigma_{2PA}(\lambda_{2PA})$		$\sigma_{2PA}'(\lambda_{2PA}')$	$\Delta\mu$
	2PEF	NLT		
<b>8</b>	GM (nm) 770 (820)	GM (nm) 1800 (820)	GM (nm) 200 (925)	D 7
<b>12</b>	NA	320 (925)	320 (925)	18 <sup>[a]</sup>
<b>15</b>	200 (800)	–	35 (925)	4
<b>16</b>	370 (790)	–	45 (900)	3
<b>19</b>	200 (790)	–	30 (900)	4
<b>20</b>	200 (790)	340 (790)	20 (890)	3

[a] Estimate of  $\Delta\mu$  for **12** is based on NLT measurement.

200 GM for **15**, **19** and **20**, 770 GM for **8**, and 370 GM for **16**; these values are in agreement with previous observations in the series of similar compounds. The increased  $\sigma_{2PA}$  for **8** and **16** compared to the other three systems correlated with the molar extinction, showing a factor of  $\approx 2$  larger peak value, as well as with a slight red shift indicative of the extended conjugation in these two systems. At longer wavelength,  $\lambda_{2PA} = 900\text{--}1000\text{ nm}$ , corresponding to the peak of the lowest-energy component of the  $S_0 \rightarrow S_1$  transition,  $\sigma_{2PA}$  varies in the range 1–100 GM. In the range 900–930 nm, that is, at an energy slightly above the 0–0 transition, **8**, **15** and **16** show a distinct peak (a shoulder in case of **19** and **20**) that may be attributed to vibronic feature amplified by the Herzberg–Teller mechanism.<sup>[29]</sup> The peak values were in the range  $\sigma_{2PA}' = 20\text{--}320\text{ GM}$ , as summarized in Table 2. Towards the very red edge of the  $S_0 \rightarrow S_1$  band, where 0–0 dominates, the  $\sigma_{2PA}$  value decreases following the linear absorption profile. Similar features were observed also in the previously studied series,<sup>[14]</sup> however, the corresponding absolute  $\sigma_{2PA}$  values were an order of magnitude smaller, supporting the above notion that the  $\text{NO}_2$  group has

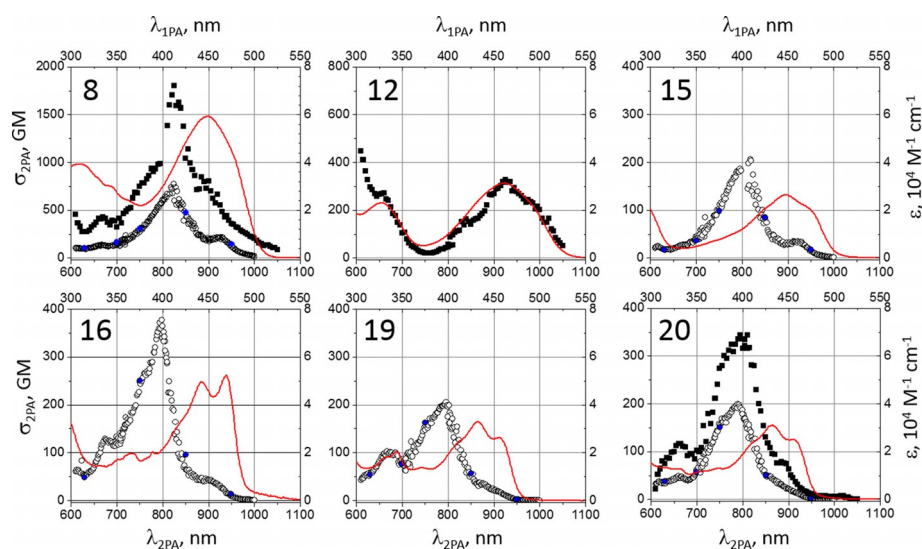


**Figure 6.** The 2PA spectra of the compounds studied in cyclohexane obtained by using the 2PEF (empty circles) and NLT (filled rectangles) methods. Filled blue circles represent wavelengths where the 2PA cross-section were evaluated using the 2PEF method. Linear absorption spectra (red solid lines) are shown for comparison. The left vertical axes represent 2PA cross-sections, right vertical axes represent extinction coefficients; bottom horizontal axes show laser (two-photon excitation) wavelengths, top horizontal axes show linear (one-photon excitation) wavelengths.

a much larger effect compared to similar but weaker electron-accepting substitutions.

The fact that no distinct 0–0 2PA peak is observed may be related to the amplification of the 0–1 band, which, along with inhomogeneous broadening, is able to mask a relatively weaker 0–0 component. For example, for 4-nitrophenyl-substituted nominally centrosymmetric porphyrins, where inhomogeneous broadening is relatively small, the 0–0 component is clearly detected in the 2PA spectrum, even though its relative amplitude can be 10–20 times less compared to the adjacent 0–1.<sup>[30]</sup> Nevertheless, the fact that 2PA did not completely vanish in the 0–0 region allowed us to assume that despite the structure being nominally centrosymmetric, the chromophores in solution may become slightly distorted, for example, due to interaction with the solvent molecules, thus rendering the two-photon transition partially allowed. The possibility of spontaneous breaking of ground- and excited-state inversion symmetry in nominally quadrupolar chromophores was suggested earlier by Terenziani et al., who considered a pseudo Jahn–Teller-type mechanism being responsible for large solvatochromism.<sup>[11]</sup> In our case, the degree by which the intrinsic symmetry may be becomes “broken” could be indirectly quantified by evaluating the ratio between  $\sigma_{2PA}$  and the linear extinction at the very red side of the spectra (i.e., at the wavelengths where the two spectral profiles coincide), using the relation:<sup>[26]</sup>

$$\Delta\mu = 4.55 \times 10^3 \left( \frac{3}{n^2 + 2} \right) \sqrt{\frac{n\sigma_{2PA}(\lambda_{2PA})}{\lambda_{2PA}\varepsilon_M(1/2\lambda_{2PA})}} \quad (1)$$

where  $\Delta\mu$  is the change of permanent electric dipole moment (in Debye),  $n$  is the solvent index of refraction,  $\lambda_{2PA}$  is the wavelength (nm),  $\varepsilon_M$  is the molar extinction coefficient ( $M^{-1} \text{ cm}^{-1}$ ), and  $\sigma_{2PA}$  is the 2PA cross-section, expressed in Göppert–Mayer units ( $1 \text{ GM} = 10^{-50} \text{ cm}^4 \text{ photon}^{-1} \text{ s}^{-1}$ ). We note that even though Equation (1) is commonly applied only to dipolar dyes,<sup>[26]</sup> there is accumulating experimental evidence that this relation may be also extended to the lowest-energy, purely electronic transition of nominally symmetric systems, where the dipole moment is created by a spontaneous symmetry breaking mechanism.<sup>[27–29]</sup> Figure 7 (top panel) shows the above dipole moment change function plotted for **8** along with the Gaussian decomposition components of the linear absorption spectrum. In the range 975–1005 nm (between vertical dotted lines, see Figure), where the longest-wavelength component dominates (presumably the 0–0 transition), the ratio between the 2PA and 1PA is constant and corresponds to the value  $\Delta\mu = 7.0 \text{ D}$ . Such a distinct dipole change suggests that the implied inversion symmetry, i.e., one following from the structure formula of the chromophore, is likely disrupted already prior to the transition to the excited state. Table 2 presents  $\Delta\mu$  values for the five fluorescent chromophores, which vary in the range 3–7 D. Recent studies have shown<sup>[31]</sup> that breaking of intrinsic molecular symmetry, which here apparently has already occurred in the ground state, may evolve and

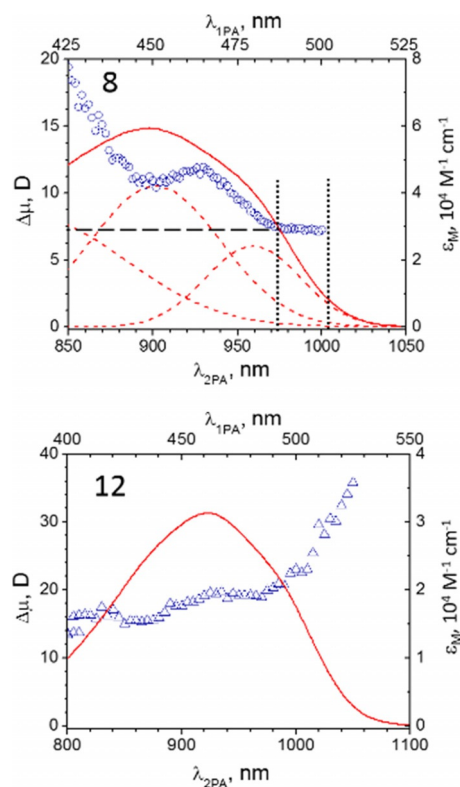


**Figure 7.** Manifestation of ground-state broken symmetry in **8** (top) and **12** (bottom) represented by non-vanishing permanent dipole moment change (symbols, left vertical axis). Linear absorption spectrum (solid line) and its Gaussian decomposition components (dashed line) are shown for comparison. The wavelengths between two vertical dotted lines is where 2PA and 1PA spectral shapes coincide, corresponding to  $\Delta\mu = 7.0 \text{ D}$  (horizontal dashed line).

expand in the excited state, where further interactions, e.g., with the solvent molecules may occur.

In the case of compound **12**, the peak 2PA measured by NLT is 320 GM. The 2-photon spectral profile essentially followed the 1-photon absorption spectrum in the  $S_0 \rightarrow S_1$  transition region. This behavior is characteristic of strongly dipolar chromophores, where parity selection rules do not apply.<sup>[31]</sup> Note that for **8** and **20**, where the NLT data is directly compared to the 2PEF measurement, the spectral shapes are closely matched, but the absolute cross-section value obtained by NLT appears as a factor 1.5–2 higher, even though both methods used fluorescein in pH 11 aqueous buffer as 2PA reference standard.<sup>[32]</sup> This discrepancy may be related to the absorption from the excited state, which effectively increases the NLT response but does not affect directly the 2PEF signal.<sup>[33]</sup> In both cases, the experimental error is on the order of 20–30%.

The bottom panel in Figure 7 shows that the dipole moment change of **12**, evaluated by inserting the experimental NLT spectrum into Equation (1), gives a value on the order 20 D. Interestingly, the dipole increases towards the longer wavelength portion of the transition band, which is likely related to a broad distribution of local electrostatic solvent environments.<sup>[19]</sup>

## Theoretical calculations

To provide a further analysis, we have used first-principle approaches to model **5**, **8**, **12**, **15**, **16**, **19** and **20**. First, given the structure of the considered dyes, we have optimized the ground-state structures of these compounds in both  $C_i$  and  $C_2$  symmetry (but for **12** which is obviously  $C_i$ ). We found that **8** and **15** are more stable in the  $C_i$  point group whereas **19** and **20** present a  $C_2$  point group, which can be understood as in these two latter compounds the side phenyl rings are arranged in a propeller-shape manner. For **16**, both  $C_i$  and  $C_2$  minima present imaginary frequencies and only the  $C_i$  structure is stable. In Table 3, we provide the dihedral angles computed

**Table 3.** Computed ground-state (GS) and lowest excited-state (ES) dihedral angles between the pyrrolo[3,2-*b*]pyrrole core and the phenyl rings bearing the nitro group(s). All values are in degree and have been computed in  $C_6H_{12}$ .

	<b>5</b>	<b>8</b>	<b>12</b>	<b>15</b>	<b>16</b>	<b>19</b>	<b>20</b>
GS	38.5	39.1	36.7	45.4	6.7	45.1	43.8
ES	26.2	23.4	33.2	34.8	6.7	36.2	34.7

between the central pyrrolo[3,2-*b*]pyrrole core and the phenyl ring bearing the nitro groups for both the ground and the excited states of all modeled compounds. For the compounds without constraints, this dihedral angle is ca. 35–40° in the ground state. In contrast, as expected it is much smaller for **16** and attains values of ca. 45° for **15**, **19** and **20**. Interestingly, this angle significantly drops, by ca. –10°, when going to the lowest excited state, an effect particularly marked for **8**. This clearly indicates an increase of the conjugation in the excited state.

The density difference plots are given for four selected compounds in Figure 8. Clearly, the central pyrrolo[3,2-*b*]pyrrole core acts as a donor moiety (mostly in blue) whereas the nitro group(s) act(s) as acceptor(s) (mostly in red), irrespective of the considered dye. In that sense, the side CN and SF<sub>5</sub> moieties added in **19** and **20** have a small impact on the excited state. This is consistent with the data of Table 1: all structures but **12** and **16** display similar positions for the absorption maximum. For **12**, one observes a significant dipolar charge-transfer (CT) character as expected, but one notices that the additional donor group plays only a small role: the pyrrolo[3,2-*b*]pyrrole core remains the main donor group. For **16**, the excited state is slightly more delocalized in line with the observed bathochromic shifts. We underline that for **12**, which is dipolar, the difference of dipole moments between the two states returned by theory is 17.6 D (excited-state dipole: 25.4 D), which is in perfect agreement with the experimentally deduced value listed in Table 2. Overall, we notice on the one hand a planarization of the structure when going from the ground to the excited state and, on the other hand, a strong reorganization of the electrons in the excited state corresponding to dipolar or quadrupolar CT effects. These trends are consistent with the large solvatochromism experimentally obtained.

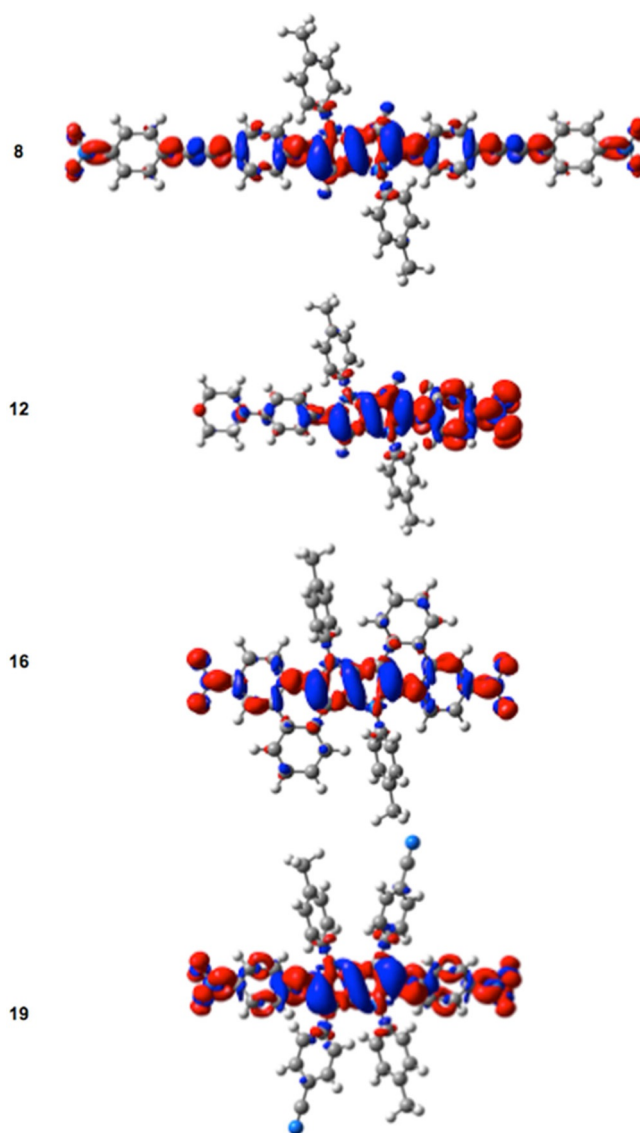


**Figure 8.** Density difference plots obtained for four compounds. In these plots, blue and red regions, respectively, indicate decrease and increase of electron density upon photon absorption (threshold used: 0.001 au).

We have determined theoretical 0–0 energies for all compounds using a protocol taking into account vibrational and solvation effects.<sup>[34]</sup> On the wavelength scale, the 0–0 points are predicted by theory to be found at 437 nm, 465 nm, 462 nm, 463 nm, 434 nm, 433 nm and 429 nm for **5**, **8**, **12**, **15**, **16**, **19** and **20**, respectively. These values can be directly compared to the crossing point between the absorption and emission spectra, and one notices that theory only slightly underestimates the absolute positions of these bands. For **16**, one notes a clear multiple peak structure in Figure 1. As the electronic excited states of **16** are well separated according to TD-DFT, we reasoned that this specific band shape was originating from vibronic contributions, which have been simulated. As can be seen in Figure 9, the calculations of vibronic effects for the lowest excited state indeed restore a multi-peak structure for absorption and the presence of a shoulder for emission. For the fluorescence, theory reproduces almost perfectly the



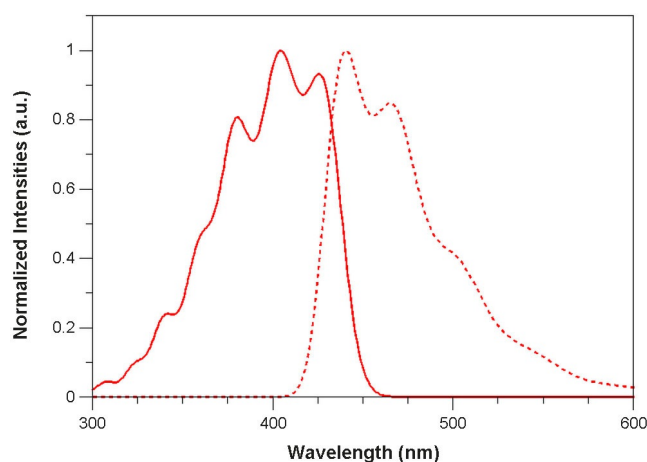


**Figure 9.** Theoretically simulated absorption (full line) and emission (dashed line) band shapes of **16**. These band topologies can be compared to their experimental counterpart given in Figure 1

experimentally observed band shape (see Figure 1), whereas for the absorption the relative intensities of the two first peaks are reversed. However, both the separation between these two peaks (ca. 0.16 eV theoretically and 0.19 eV experimentally) and the molar absorption coefficient (theory:  $42\,400\text{ M}^{-1}\text{ cm}^{-1}$ , experiment:  $52\,300\text{ M}^{-1}\text{ cm}^{-1}$ ) are confirming the quality of theoretical modeling and, therefore, the vibronic origin of the specific band shape of **16**. Eventually for the dipolar **12**, we have also used TD-DFT to determine the 2PA cross-section and obtained a value of 439 GM for the first absorption band, a value that is reasonably close to the one obtained by the measurement (see Table 2).

## Conclusions

In summary, we have presented a concept for modulating the excited-state process by changing the dihedral angle between electron-withdrawing peripheral subunits and the electron-rich pyrrolo[3,2-*b*]pyrrole core. Regardless of the degree of conjugation between the nitrobenzene moieties and the pyrrolo[3,2-*b*]pyrrole core, the centrosymmetric dyes of this type displayed solvatofluorochromism when the dihedral angle is variable. Suppression of this phenomenon could be achieved via planarization of the molecule, which was synthetically achieved via oxidative aromatic coupling. This suppression suggests that the difference between the conformation in the ground and excited states is important for molecular orbital desymmetrization after electronic excitation. All these nominally quadrupolar heterocycles possessed strong emission in cyclohexane ( $\geq 0.25$ ), while this fluorescence was lost upon switching to a dipolar architecture. Upon  $\pi$ -expansion of the chromophore by means of additional carbon-carbon triple bonds, the emission intensity decreased while the large solvatofluorochromism effect was retained. This data suggests that non-planar dyes exhibit an increased preference for planarity in the excited state. Interestingly, all studied pyrrolo[3,2-*b*]pyrroles possess red fluorescence in the solid state. Measurement of femtosec-

ond two-photon absorption in the 0-0 component of the  $S_0 \rightarrow S_1$  transition revealed that not only the nonsymmetric system has a large permanent electric dipole moment change upon the transition to the excited state, but also that the nominally symmetric structures exhibit a non-vanishing, permanent dipole, thus suggesting that some degree of symmetry breaking may occur already prior to solvent-induced symmetry breaking in the excited state. These findings reveal the generality of solvatofluorochromism of centrosymmetric pyrrolo[3,2-*b*]pyrroles possessing a center of inversion and provide a potential platform for translation of this molecular design to various applications.

## Experimental Section

### Synthesis

All chemicals were used as received (Aldrich and TCI) unless otherwise noted. Reagent grade solvents ( $\text{CH}_2\text{Cl}_2$ , hexane, toluene) were distilled prior to use. All reported  $^1\text{H}$  NMR and  $^{13}\text{C}$  NMR spectra were recorded on Varian 500 and 600 MHz instruments. Chemical shifts ( $\delta$ ) were determined with TMS as the internal reference; *J* values were given in Hz. Chromatography was performed on silica (Kieselgel 60, 200–400 mesh).

**Synthesis of compound (6):** 4-Octylaniline (2.46 g, 12 mmol), 4-[(trimethylsilyl)ethynyl]benzaldehyde (2.43 g, 12 mmol) and *p*-toluenesulfonic acid (228 mg, 1.2 mmol) were stirred in glacial acetic acid (10 mL) at 90 °C for 30 min. Then, butane-2,3-dione (519  $\mu\text{L}$ , 6 mmol) was added and the resulting mixture was stirred at 90 °C for 3 h. After cooling, the precipitate was filtered off and washed with glacial acetic acid. Recrystallization from EtOAc afforded the pure product as a yellow solid (553 mg, 11%).  $R_f = 0.4$  (silica, hexanes/ $\text{CH}_2\text{Cl}_2$  7:3);  $^1\text{H}$  NMR (500 MHz,  $\text{CDCl}_3$ ):  $\delta = 0.23$  (s, 18H), 0.89 (t,  $J = 7.0$  Hz, 6H) 1.29–1.33 (m, 20H), 1.62–1.64 (m, 4H), 2.61 (t,  $J = 7.6$  Hz, 4H), 6.39 (s, 2H), 7.12 (AA'XX',  $J = 8.6$  Hz, 4H), 7.15 (s, 8H), 7.30 ppm (AA'XX',  $J = 8.6$  Hz, 4H);  $^{13}\text{C}$  NMR (125 MHz,  $\text{CDCl}_3$ ):  $\delta = 14.1, 22.7, 29.2, 29.3, 31.3, 35.5, 76.7, 77.0, 77.2, 94.5, 94.8, 105.3, 120.2, 125.1, 127.5, 129.1, 131.7, 132.4, 133.7, 135.5, 137.4, 140.7$  ppm; HR MS (EI) calcd for  $\text{C}_{56}\text{H}_{70}\text{N}_2\text{Si}_2$ : 826.5078, found 826.5086; m.p. 180–181 °C.

**Synthesis of compound (7):** The TMS-protected derivative (**6**, 500 mg, 0.6 mmol) was dissolved in THF (3.4 mL) and TBAF·3H<sub>2</sub>O (392 mg, 1.5 mmol) was added. The reaction mixture was stirred for 5 h at rt. The solvent was evaporated and the crude product was recrystallized from EtOAc. The pure product was obtained as a yellow solid (294 mg, 72%).  $R_f = 0.4$  (silica, hexanes/ $\text{CH}_2\text{Cl}_2$  7:3);  $^1\text{H}$  NMR (500 MHz,  $\text{CDCl}_3$ ):  $\delta = 0.89$  (t,  $J = 7.0$  Hz, 6H), 1.28–1.33 (m, 20H), 1.61–1.66 (m, 4H), 2.62 (t,  $J = 7.7$  Hz, 4H), 3.06 (s, 2H), 6.40 (s, 2H), 7.15 (AA'XX' overlap, 4H), 7.17 (s, 8H), 7.35 ppm (AA'XX',  $J = 8.4$  Hz, 4H);  $^{13}\text{C}$  NMR (125 MHz,  $\text{CDCl}_3$ ):  $\delta = 14.1, 22.7, 29.2, 29.3, 29.4, 31.3, 31.9, 35.5, 76.7, 77.0, 77.2, 77.4, 83.8, 94.9, 119.2, 125.1, 127.6, 129.1, 131.9, 132.4, 134.1, 135.4, 137.4, 140.8$  ppm; HR MS (EI) calcd for  $\text{C}_{50}\text{H}_{54}\text{N}_2$ : 682.4287, found 682.4293; m.p. 183–184 °C.

**Synthesis of compound (8):** A dried Schlenk flask, purged with argon, was charged with **7** (50 mg, 0.073  $\mu\text{mol}$ ) and 1-iodo-4-nitrobenzene (36.4 mg, 0.146 mmol). The substrates were dissolved in anhydrous THF (1 mL). Then,  $\text{Et}_3\text{N}$  (0.1 mL, 7.2 mmol) was added. The vessel was evacuated and backfilled with argon (this process was repeated 3 times). To the degassed mixture, CuI (1.4 mg, 7.3  $\mu\text{mol}$ ) and  $\text{PdCl}_2(\text{PPh}_3)_2$  (5 mg, 7.3  $\mu\text{mol}$ ) were added. The reaction mixture was stirred at rt for 20 h. Next, the reaction mixture

was filtered through a short pad of Celite, and evaporated to dryness. The crude product was chromatographed (silica, hexanes/CH<sub>2</sub>Cl<sub>2</sub> 7:3) to afford orange product **8** (50 mg, 74%). *R*<sub>f</sub>=0.67 (silica, hexanes/CH<sub>2</sub>Cl<sub>2</sub> 7:3); <sup>1</sup>H NMR (500 MHz, CDCl<sub>3</sub>): δ = 0.89 (t, *J* = 7.0 Hz, 6H), 1.26–1.34 (m, 20H), 1.68–1.62 (m, 4H), 2.64 (t, *J* = 7.6 Hz, 4H), 6.45 (s, 2H), 7.20 (s, 8H), 7.23 (AA'XX', *J* = 8.3 Hz, 4H), 7.39 (AA'XX', *J* = 8.3 Hz, 4H), 7.62 (d, *J* = 8.9 Hz, 4H), 8.21 ppm (d, *J* = 8.9 Hz, 4H); <sup>13</sup>C NMR (125 MHz, CDCl<sub>3</sub>): δ = 14.1, 22.7, 29.3, 29.3, 29.4, 31.3, 31.9, 35.5, 76.7, 77.0, 77.2, 88.2, 95.2, 119.2, 123.6, 125.1, 127.7, 129.2, 130.4, 131.6, 132.1, 132.8, 134.5, 135.5, 137.3, 141.0, 146.8 ppm; LR MS (EI) calcd for C<sub>62</sub>H<sub>60</sub>N<sub>4</sub>O<sub>4</sub>: 924.46, found 924.46; m.p. 234 °C.

**Synthesis of compound (10):** 4-Octylaniline (2.05 g, 10 mmol), 4-nitrobenzaldehyde (756 mg, 5 mmol), 4-bromobenzaldehyde (925 mg, 5 mmol) and *p*-toluenesulfonic acid (190 mg, 1 mmol) were stirred in glacial acetic acid (10 mL) at 90 °C for 30 min. Then, butane-2,3-dione (432 μL, 6 mmol) was added and the resulting mixture was stirred at 90 °C for 3 h. After cooling, the precipitate was filtered off and washed with glacial acetic acid. The crude product was chromatographed (silica, hexanes/toluene 6:4) to afford an orange product **10** (600 mg, 16%). *R*<sub>f</sub>=0.65 (silica, hexanes/CH<sub>2</sub>Cl<sub>2</sub> 7:3); <sup>1</sup>H NMR (500 MHz, CDCl<sub>3</sub>): δ = 0.89 (t, *J* = 6.9 Hz, 6H), 1.31 (m, 20H), 1.64 (m, 4H), 2.64 (q, *J* = 6.6, 8.7 Hz, 4H), 6.34 (s, 1H), 6.54 (s, 1H), 7.08 (AA'XX', *J* = 8.6 Hz, 2H), 7.14–7.22 (m, 8H), 7.31 (dd, *J* = 22.7, 8.8 Hz, 4H), 8.03 ppm (AA'XX', *J* = 8.6 Hz, 2H); <sup>13</sup>C NMR (125 MHz, CDCl<sub>3</sub>): δ = 14.1, 22.7, 29.3, 29.3, 29.4, 29.5, 31.3, 31.9, 35.5, 76.8, 77.0, 77.3, 94.3, 96.8, 120.5, 123.7 ppm; HR MS (EI) calcd for C<sub>46</sub>H<sub>52</sub>BrN<sub>3</sub>O<sub>2</sub>: 757.3243, found 757.3248; m.p. 214–215 °C.

**Synthesis of compound (12):** A dried Schlenk flask, purged with argon, was charged with **10** (350 mg, 0.25 mmol). Compound **10** was then dissolved in anhydrous toluene (14 mL) and morpholine (**11**) (70 μL, 0.805 mmol) was added, followed by Cs<sub>2</sub>CO<sub>3</sub> (514 mg, 1.58 mmol). The vessel was evacuated and backfilled with argon (this process was repeated 3 times). Next, SPhos (21.6 mg, 0.0526 mmol) was added. The reaction mixture was stirred at 120 °C for 18 h. Afterwards, the reaction mixture was filtered through a pad of Celite and evaporated to dryness. The crude product was chromatographed (silica, toluene) to obtain a dark violet product **12** (342 mg, 85%). *R*<sub>f</sub>=0.36 (silica, CH<sub>2</sub>Cl<sub>2</sub>/hexanes 1:1); <sup>1</sup>H NMR (500 MHz, CDCl<sub>3</sub>): δ = 0.89 (t, *J* = 6.9 Hz, 6H), 1.13–1.43 (m, 20H), 1.62–1.66 (m, 4H), 2.61–2.66 (m, 4H), 3.22–3.10 (m, 4H), 3.14 (t, *J* = 4.4 Hz, 4H), 3.84 (t, *J* = 4.4 Hz, 4H), 6.27 (s, 1H), 6.56 (s, 1H), 6.77 (d, *J* = 8.4 Hz, 2H), 7.13 (d, *J* = 8.7 Hz, 2H), 7.18–7.23 (m, 4H), 7.27 (d, *J* = 8.9 Hz, 2H), 8.02 ppm (d, *J* = 8.9 Hz, 2H); <sup>13</sup>C NMR (125 MHz, CDCl<sub>3</sub>): δ = 14.1, 22.7, 22.7, 29.3, 29.3, 29.3, 29.4, 29.5, 31.3, 31.9, 35.5, 48.9, 66.8, 76.7, 77.0, 77.3, 93.0, 97.1, 115.0, 123.7, 124.8, 125.1, 125.2, 127.0, 129.0, 129.2, 129.4, 131.4, 131.4, 132.6, 134.5, 134.5, 137.3, 137.4, 138.4, 140.2 ppm; HR MS (EI) calcd for C<sub>50</sub>H<sub>60</sub>N<sub>4</sub>O<sub>3</sub>: 764.4665, found 764.4664; m.p. 158 °C.

**Synthesis of compound (14):** 4-Octylaniline (1.03 g, 5 mmol), 2-bromo-4-nitrobenzaldehyde (1.15 g, 5 mmol) and *p*-TsOH (95 mg, 0.5 mmol) were stirred in glacial acetic acid (5 mL) at 90 °C for 30 min. Then, butane-2,3-dione (216 μL, 2.5 mmol) was added and the resulting mixture was stirred at 90 °C for 3 h. After cooling, the precipitate was filtered off and washed with glacial acetic acid. Recrystallization from EtOAc afforded the pure product as an orange solid (850 mg, 19%). *R*<sub>f</sub>=0.7 (silica, CH<sub>2</sub>Cl<sub>2</sub>/hexanes 1:1); <sup>1</sup>H NMR (500 MHz, CDCl<sub>3</sub>): δ = 0.88 (t, *J* = 6.9 Hz, 6H), 1.34–1.22 (m, 20H), 1.58–1.62 (m, 4H), 2.59 (t, *J* = 7.7 Hz, 4H), 6.64 (s, 2H), 7.08 (d, *J* = 8.4 Hz, 4H), 7.14 (d, *J* = 8.4 Hz, 4H), 7.30 (d, *J* = 8.6 Hz, 2H), 8.00 (dd, *J* = 8.6, 2.3 Hz, 2H), 8.47 ppm (d, *J* = 2.3 Hz, 2H); <sup>13</sup>C NMR (125 MHz, CDCl<sub>3</sub>): δ = 14.1, 22.7, 29.3, 29.3, 29.4, 31.2, 31.9, 35.4, 97.9, 121.7, 123.5, 124.2, 128.6, 129.3, 131.5, 132.6, 132.8, 136.6,

141.0, 141.1, 146.4 ppm; HR MS (EI) calcd for C<sub>46</sub>H<sub>50</sub>BrN<sub>4</sub>O<sub>4</sub>: 880.2199, found 880.2205; m.p. 197–198 °C.

**Synthesis of compound (15):** A Schlenk flask was charged with **13** (221 mg, 0.25 mmol), and phenylboronic acid (92 mg, 0.75 mmol), PPh<sub>3</sub> (26 mg, 0.1 mmol), K<sub>2</sub>CO<sub>3</sub> (138 mg, 1 mmol), and Pd(OAc)<sub>2</sub> (11 mg, 0.05 mmol) were added. The substrates were dissolved in toluene (0.2 mL) and water (0.2 mL). The reaction mixture was stirred at 80 °C for 4 days. Then, the reaction mixture was filtered through a short pad of Celite, and evaporated. The crude product was chromatographed (silica, hexanes/CH<sub>2</sub>Cl<sub>2</sub> 2:8), affording orange product **15** (161 mg, 73%). *R*<sub>f</sub>=0.4 (silica, CH<sub>2</sub>Cl<sub>2</sub>/hexanes 1:1); <sup>1</sup>H NMR (600 MHz, CDCl<sub>3</sub>): δ = 0.90 (t, *J* = 7.0 Hz, 6H), 1.26–1.38 (m, 20H), 1.56–1.65 (m, 4H), 2.53 (t, *J* = 7.6 Hz, 4H), 6.25 (s, 2H), 6.44 (d, *J* = 8.3 Hz, 4H), 6.67 (dd, *J* = 8.2, 1.0 Hz, 4H), 6.84 (d, *J* = 8.3 Hz, 4H), 7.07 (t, *J* = 7.7 Hz, 4H), 7.19 (t, *J* = 7.4 Hz, 2H), 7.73 (d, *J* = 8.5 Hz, 2H), 8.06 (d, *J* = 2.4 Hz, 2H), 8.20 ppm (dd, *J* = 8.5, 2.4 Hz, 2H); <sup>13</sup>C NMR (150 MHz, CDCl<sub>3</sub>): δ = 14.1, 22.7, 29.3, 29.3, 29.5, 31.7, 31.9, 35.36, 76.79, 96.8, 122.2, 122.8, 125.3, 127.1, 127.9, 128.1, 128.7, 131.1, 131.5, 133.3, 136.2, 138.7, 139.2, 139.9, 141.7, 147.0 ppm; HR MS (EI) calcd for C<sub>58</sub>H<sub>60</sub>N<sub>4</sub>O<sub>4</sub>: 876.4615, found 876.4581; m.p. 197 °C.

**Synthesis of compound (16):** A Schlenk flask flushed with argon was charged with **15** (100 mg, 0.11 mmol) which was dissolved in dry CH<sub>2</sub>Cl<sub>2</sub> (1.32 mL). Then, a solution of FeCl<sub>3</sub> (370 mg, 2.28 mmol) dissolved in nitromethane (1.32 mL) was added via syringe. The reaction was stirred 40 min at rt. Then, water (1.5 mL) was added and the resulting mixture was stirred for another 15 min. Two phases were separated and the water phase was extracted with CH<sub>2</sub>Cl<sub>2</sub> (3 × 10 mL). The organic phases were combined and dried, the solvent was evaporated, and the crude product was chromatographed (silica, CH<sub>2</sub>Cl<sub>2</sub>/hexanes 8:2) to afford an orange product **16** (66 mg, 69%). *R*<sub>f</sub>=0.45 (silica, CH<sub>2</sub>Cl<sub>2</sub>/hexanes 1:1); <sup>1</sup>H NMR (500 MHz, CDCl<sub>3</sub>): δ = 0.94 (t, *J* = 7.0 Hz, 6H), 1.46–1.65 (m, 20H), 1.91 (t, *J* = 7.2 Hz, 4H), 2.97 (t, *J* = 7.5 Hz, 4H), 6.89 (d, *J* = 8.2 Hz, 2H), 7.10 (t, *J* = 7.6 Hz, 2H), 7.49 (t, *J* = 7.5 Hz, 2H), 7.56 (d, *J* = 9.4 Hz, 2H), 7.61 (d, *J* = 7.8 Hz, 4H), 7.72 (d, *J* = 7.8 Hz, 4H), 8.01 (d, *J* = 9.4 Hz, 2H), 8.72 (d, *J* = 8.2 Hz, 2H), 9.62 ppm (s, 2H); <sup>13</sup>C NMR (125 MHz, CDCl<sub>3</sub>): δ = 14.2, 22.7, 29.4, 29.4, 29.6, 31.9, 32.0, 36.0, 110.6, 119.8, 119.9, 122.8, 123.5, 124.7, 126.6, 127.1, 127.4, 128.2, 129.4, 130.5, 130.6, 132.0, 133.4, 140.1, 143.7, 146.1 ppm; HR MS (EI) calcd for C<sub>58</sub>H<sub>56</sub>N<sub>4</sub>O<sub>4</sub>: 872.4301, found 872.4289; m.p. 296 °C.

**Synthesis of compound (19):** 2,5-Bis-(4-nitrophenyl)-1,4-bis(4-octylphenyl)-1,4-dihydropyrrolo[3,2-*b*]pyrrole **5** (181 mg, 0.25 mmol), 4-bromobenzonitrile (182 mg, 1 mmol), KOAc (98 mg, 1 mmol), and PdCl(C<sub>3</sub>H<sub>5</sub>)(dppb) (6 mg, 0.01 mmol) were placed in a Schlenk flask, which was flushed with argon prior to use. Then, 8 mL of dry DMA was added and the resulting mixture was stirred at 150 °C for 5 days. The crude product was chromatographed (silica, hexanes/CH<sub>2</sub>Cl<sub>2</sub> 2:8) to afford **19** as an orange product (162 mg, 70%). *R*<sub>f</sub>=0.48 (silica, CH<sub>2</sub>Cl<sub>2</sub>/hexanes 1:1); <sup>1</sup>H NMR (500 MHz, CDCl<sub>3</sub>): δ = 0.90 (t, *J* = 7.0 Hz, 6H), 1.28–1.36 (m, 20H), 1.55–1.60 (m, 4H), 2.57 (t, *J* = 7.7 Hz, 4H), 6.79 (dd, *J* = 14.6, 8.2 Hz, 8H), 6.91 (d, *J* = 8.2 Hz, 4H), 7.00 (d, *J* = 8.8 Hz, 4H), 7.20 (d, *J* = 8.2 Hz, 4H), 7.91 ppm (d, *J* = 8.8 Hz, 4H); <sup>13</sup>C NMR (125 MHz, CDCl<sub>3</sub>): δ = 14.1, 22.6, 29.2, 29.3, 29.3, 31.6, 31.8, 35.4, 108.7, 109.7, 118.6, 123.2, 127.5, 128.8, 129.4, 131.0, 131.2, 131.3, 132.8, 135.2, 137.8, 143.2, 146.2 ppm; LR MS (ES) calcd for C<sub>60</sub>H<sub>58</sub>N<sub>6</sub>O<sub>4</sub>: 926.45, found 926.46; m.p. 271–273 °C.

**Synthesis of compound (20):** 2,5-Bis-(4-nitrophenyl)-1,4-bis(4-octylphenyl)-1,4-dihydropyrrolo[3,2-*b*]pyrrole **5** (100 mg, 0.137 mmol), 4-bromophenylsulfur pentafluoride (156 mg, 0.551 mmol), KOAc (54 mg, 0.551 mmol), and PdCl(C<sub>3</sub>H<sub>5</sub>)(dppb) (3.3 mg, 5.51 μmol) were placed in a Schlenk flask, which was flushed with argon prior to use. Then, 4.6 mL of dry DMA was added and the resulting mixture

ture was stirred at 130 °C for 3 days. The product was purified by means of flash column chromatography (eluent: 10% EtOAc in hexane) and then recrystallized from toluene or ethyl acetate. The obtained orange crystals were dried under reduced pressure (109 mg, 70%).  $R_f=0.4$  (silica,  $\text{CH}_2\text{Cl}_2/\text{hexanes}$  1:1);  $^1\text{H NMR}$  ( $\text{CDCl}_3$ , 500 MHz, 25 °C):  $\delta=0.89$  (t,  $J=7.0$  Hz, 6H), 1.34–1.30 (m, 20H), 1.56–1.53 (m, 4H), 2.53 (t,  $J=7.8$  Hz, 4H), 6.75 (d,  $J=8.3$  Hz, 4H), 6.78 (d,  $J=8.5$  Hz, 4H), 6.89 (d,  $J=8.5$  Hz, 4H), 7.04 (AA'XX',  $J=9.0$  Hz, 4H), 7.30 (d,  $J=8.5$  Hz, 4H), 7.92 ppm (AA'XX',  $J=9.0$  Hz, 4H);  $^{13}\text{C NMR}$  ( $\text{CDCl}_3$ , 125 MHz, 25 °C)  $\delta$  14.1, 22.6, 29.2, 29.3, 29.4, 31.4, 31.9, 35.4, 108.4, 123.3, 125.2, 127.5, 128.8, 129.7, 130.5, 131.2, 151.8, 146.1, 143.2, 137.9, 136.6, 135.2, 132.6 ppm; LRMS: (ESI): calcd for  $\text{C}_{58}\text{H}_{59}\text{F}_{10}\text{N}_4\text{O}_4\text{S}_2$   $[\text{M} + \text{H}]^+$ : 1129.22, found: 1129.38; m.p. 278–280 °C.

## Optical measurements

Spectroscopic samples were prepared in 2 mL quartz cuvettes of 1 cm path length for both 1PA and 2PA measurements. Cyclohexane (FisherChemicals, UN 1145, HPLC grade, 99.9%) and dichloromethane (OmniSolv, UN 1593, DX 0831-6, 99.96%) were used. Linear absorption measurements were performed with a PerkinElmer UV/VIS/NIR Lambda 950 spectrometer. For relative quantum yield measurements (for the 2PEF measurements), a luminescence PerkinElmer LS 50B spectrometer was used. The sample concentrations used in the 2PEF measurements were  $\approx 1 \mu\text{M}$ , while for the NLT measurements higher concentrations of  $\approx 1\text{--}4 \text{ mM}$  were required. For samples with high quantum yields, the relative 2PA spectra were obtained using the 2PEF method. A Ti:Sapphire femtosecond laser system (Coherent, Libra) operated at 1 kHz repetition rate and producing pulses with duration  $\approx 100$  fs pumped an optical parametric amplifier (1PA) (Light Conversion, OPerA Solo). The 1PA output wavelength was tuned in the wavelength region 570–900 nm with 2 nm steps. The approximate 1PA pulse spectral width was  $\approx 15\text{--}35$  nm. For detection of the fluorescent signal, a grating spectrometer (Jobin–Yvon, Triax 550) combined with a CCD detector (Spectrum One) was used. Bis-diphenylaminostilbene (bDPAS) diluted in dichloromethane was used as the reference standard for the 2PEF measurements.<sup>[35]</sup> When the fluorescence quantum yields were too low for reliable 2PEF measurements, the femtosecond NLT method was used to determine the 2PA cross-sections in a range of 570–800 nm.<sup>[36]</sup> Briefly, for the NLT measurements, the same laser setup was employed, but the pulse repetition rate was reduced to 100 Hz. The 1PA beam was additionally collimated using a series of apertures and lenses. To detect the change in the transmission, a set of silicon photodetectors (Thorlabs, DET 36A) was employed. Bis-diphenylaminodistyrilbenzene (bDPASDSB) diluted in tetrahydrofuran (OmniSolv, UN 2056, TX 0279-1, 99.9%) was used as the reference standard for the NLT measurements.

**Theoretical calculations:** All (TD)-DFT calculations were performed using the Gaussian 09.D01 program,<sup>[37]</sup> whereas the 2PA calculations were performed in the Dalton code.<sup>[38]</sup> For the Gaussian calculations, we used tightened self-consistent field ( $10^{-10}$  a.u.) and geometry optimization ( $10^{-5}$  a.u.) convergence thresholds and a large DFT integration grid (so-called ultrafine grid, a pruned 99590 grid). The linear optical spectra (TD)-DFT calculations relied on the M06-2X hybrid functional.<sup>[39]</sup> This functional is known to provide slightly excessive transition energies but provided consistent data (high correlation) with the experiment. Following the basis set combination approach proposed elsewhere,<sup>[40]</sup> we used the 6-31+G(d) atomic basis set for determining the geometrical and vibrational parameters, whereas the transition energies were computed with 6-311+G(2d,p). The nature of the ground-state sta-

tionary points was confirmed by analytical Hessian calculations that returned 0 (minima) imaginary vibrational modes. Environmental effects (herein, of cyclohexane) were accounted for using the linear response (LR) variant of the polarizable continuum model (PCM)<sup>[41]</sup> in its non-equilibrium limit for the vertical absorption. For the emission wavelengths, the excited-state structures were optimized with the LR-PCM in its equilibrium limit, whereas the emission energies were computed with the corrected LR (cLR)<sup>[42]</sup> PCM model in its non-equilibrium limit. Excited-states are represented using density difference plots, in which the excited-state density was determined at the TD-DFT level using the Z-vector approach. Vibrationally resolved spectra have been obtained using the FCclasses program.<sup>[43]</sup> The Franck-Condon (FC) approximation has been employed as we consider strongly dipole-allowed transitions ( $f > 0.1$ ).<sup>[44]</sup> The reported spectra have been simulated by using convoluting Gaussian functions having a half width at half-maximum (HWHM) of 0.07 eV. A maximum number of 25 overtones for each mode and 20 combination bands on each pair of modes were included in the calculation. The number of integrals to be computed for each class was set to 1011, which gives FC factors of 0.67 and 0.78 for the absorption and emission of 16, respectively. The 2PA calculations were performed in the gas-phase using the range-separated CAM-B3LYP functional<sup>[45]</sup> which is suited for nonlinear optical calculations. We applied the diffuse containing 6-31+G(d,p) atomic basis set for the 2PA simulations.

## Acknowledgements

We thank Global Research Laboratory Program (2014K1A1A2064569) through the National Research Foundation (NRF) funded by Ministry of Science, ICT & Future Planning (Korea) and the National Science Centre, Poland (Grant MAESTRO-2012/06/A/ST5/00216). A.R. and A.M. acknowledge AFOSR Grant FA9550-16-1-0189 and A.R. support by the Estonian Institutional Research grant IUT-23 and European Regional Development Fund project TK134. C. A. thanks the Agence Nationale de la Recherche for supporting her PhD (EMA grant). D.J. acknowledges the Region des Pays de la Loire for constant support. This work used computational resources from the CCIPL, the CINES and the local Troy cluster.

## Conflict of interest

The authors declare no conflict of interest.

**Keywords:** donor–acceptor systems • dyes/pigments • fluorescence • fused-ring systems • structure–activity relationship

- [1] a) B. A. Reinhardt, L. L. Brott, S. J. Clarson, A. G. Dillard, J. C. Bhatt, R. Kannan, L. Yuan, G. S. He, P. N. Prasad, *Chem. Mater.* **1998**, *10*, 1863; b) M. Albota, D. Beljonne, J. L. Bredas, J. E. Ehrlich, J. Y. Fu, A. A. Heikal, S. E. Hess, T. Kogej, M. D. Levin, S. R. Marder, D. McCord-Maughon, J. W. Perry, H. Rockel, M. Rumi, G. Subramaniam, W. W. Webb, X. L. Wu, C. Xu, *Science* **1998**, *281*, 1653–1656; c) T. K. Ahn, K. S. Kim, D. Y. Kim, S. B. Noh, N. Aratani, C. Ikeda, A. Osuka, D. Kim, *J. Am. Chem. Soc.* **2006**, *128*, 1700–1704; d) M. Williams-Harry, A. Bhaskar, G. Ramakrishna, T. Goodson III, M. Imamura, A. Mawatari, K. Nakao, H. Enozawa, T. Nishinaga, M. Iyoda, *J. Am. Chem. Soc.* **2008**, *130*, 3252–3253; e) D. Yan, *Chem. Eur. J.* **2015**, *21*, 4880–4896; f) K. Kamada, S.-I. Fuku-en, S. Minamide, K. Ohta,

- R. Kishi, M. Nakano, H. Matsuzaki, H. Okamoto, H. Higashikawa, K. Inoue, S. Kojima, Y. Yamamoto, *J. Am. Chem. Soc.* **2013**, *135*, 232–241; g) D. Yan, A. Delori, G. O. Lloyd, T. Friščić, G. M. Day, W. Jones, J. Lu, M. Wei, D. G. Evans, X. Duan, *Angew. Chem. Int. Ed.* **2011**, *50*, 12483–12486; *Angew. Chem.* **2011**, *123*, 12691–12694.
- [2] a) K. D. Belfield, M. V. Bondar, S. Yao, I. A. Mikhailov, V. S. Polikanov, O. V. Przhonska, *J. Phys. Chem. C* **2014**, *118*, 13790–13800; b) H. M. Kim, B. R. Cho, *Acc. Chem. Res.* **2009**, *42*, 863–872; c) A. S. Rao, D. Kim, H. Nam, H. Jo, K. H. Kim, C. Ban, K. H. Ahn, *Chem. Commun.* **2012**, *48*, 3206–3208; d) B. R. Cho, M. J. Piao, K. H. Son, H. L. Sang, J. Y. Soo, S.-J. Jeon, M. Cho, *Chem. Eur. J.* **2002**, *8*, 3907–3916.
- [3] E. J. Cueto Díaz, S. Picard, V. Chevasson, J. Daniel, V. Hugues, O. Mongin, E. Genin, M. Blanchard-Desce, *Org. Lett.* **2015**, *17*, 102–105.
- [4] C. Tang, Q. Zheng, H. Zhu, L. Wang, S.-C. Chen, E. Ma, X. Chen, *J. Mater. Chem. C* **2013**, *1*, 1771–1780.
- [5] D. A. Parthenopoulos, P. M. Renzepis, *Science* **1989**, *245*, 843–845; C. C. Corredor, Z.-L. Huang, K. D. Belfield, A. R. Morales, M. V. Bondar, *Chem. Mater.* **2007**, *19*, 5165–5173.
- [6] F. Claeysens, E. A. Hasan, A. Gaidukeviciute, D. S. Achilleos, A. Ranella, C. Reinhardt, A. Ovsianikov, X. Shizhou, C. Fotakis, M. Vamvakaki, B. N. Chichkov, M. Farsari, *Langmuir* **2009**, *25*, 3219–3223.
- [7] a) D. Yan, W. Jones, G. Fan, M. Wei, D. G. Evans, *J. Mater. Chem. C* **2013**, *1*, 4138–4145; b) S. K. Lee, W. J. Yang, J. J. Choi, C. H. Kim, S.-J. Jeon, B. R. Cho, *Org. Lett.* **2005**, *7*, 323–326; c) M. Grzybowski, V. Hugues, M. Blanchard-Desce, D. T. Gryko, *Chem. Eur. J.* **2014**, *20*, 12493–12501; d) S. Zheng, A. Leclercq, J. Fu, L. Beverina, L. A. Padilha, E. Zojer, K. Schmidt, S. Barlow, J. Luo, S.-H. Jiang, A. K.-Y. Jen, Y. Yi, Z. Shuai, E. W. Van Stryland, D. J. Hagan, J.-L. Brédas, S. R. Marder, *Chem. Mater.* **2007**, *19*, 432–442; e) K. Susumu, J. A. N. Fisher, J. Zheng, D. N. Beratan, A. G. Yodh, M. J. Therien, *J. Phys. Chem. A* **2011**, *115*, 5525–5539; f) A. Nowak-Król, M. Grzybowski, J. Romiszewski, M. Drobizhev, G. Wicks, M. Chotkowski, A. Rebane, E. Górecka, D. T. Gryko, *Chem. Commun.* **2013**, *49*, 8368–8370.
- [8] a) M. Rumi, J. E. Ehrlich, A. A. Heikal, J. W. Perry, S. Barlow, Z. Hu, D. McCord-Maughon, T. C. Parker, H. Röckel, S. Thayumanavan, S. R. Marder, D. Beljonne, J.-L. Brédas, *J. Am. Chem. Soc.* **2000**, *122*, 9500–9510; b) H. Y. Woo, B. Liu, B. Kohler, D. Korystov, A. Mikhailovsky, G. C. Bazan, *J. Am. Chem. Soc.* **2005**, *127*, 14721–14729; c) S. J. K. Pond, M. Rumi, M. D. Levin, T. C. Parker, D. Beljonne, M. W. Day, J.-L. Brédas, S. R. Marder, J. W. Perry, *J. Phys. Chem. A* **2002**, *106*, 11470–11480; d) Z.-Q. Liu, Q. Fang, D.-X. Cao, D. Wang, G.-B. Xu, *Org. Lett.* **2004**, *6*, 2933–2936; e) D. Yan, G. Fan, Y. Guan, Q. Meng, C. Li, J. Wang, *Phys. Chem. Chem. Phys.* **2013**, *15*, 19845–19852; f) M. Tasiar, V. Hugues, M. Blanchard-Desce, D. T. Gryko, *Chem. Asian J.* **2012**, *7*, 2656–2661; g) A. Purc, K. Sobczyk, Y. Sakagami, A. Ando, K. Kamada, D. T. Gryko, *J. Mater. Chem. C* **2015**, *3*, 742–749; h) M. Grzybowski, E. Glodkowska-Mrowka, V. Hugues, W. Brutkowski, M. Blanchard-Desce, D. T. Gryko, *Chem. Eur. J.* **2015**, *21*, 9101–9110; i) Y. Iwase, K. Kamada, K. Ohta, K. Kondo, *J. Mater. Chem.* **2003**, *13*, 1575–1581; j) W. R. Zipfel, R. M. Williams, R. Christie, A. Y. Nikitin, B. T. Hyman, W. W. Webb, *Proc. Natl. Acad. Sci. USA* **2003**, *100*, 7075–7080; k) D. Yan, H. Yang, Q. Meng, H. Lin, M. Wei, *Adv. Funct. Mater.* **2014**, *24*, 587–594.
- [9] a) M. Pawlicki, H. A. Collins, R. G. Denning, H. L. Anderson, *Angew. Chem. Int. Ed.* **2009**, *48*, 3244–3266; *Angew. Chem.* **2009**, *121*, 3292–3316; b) H. M. Kim, B. R. Cho, *Chem. Rev.* **2015**, *115*, 5014–5055.
- [10] a) P. Hrobárik, V. Hrobáriková, I. Sigmundová, P. Zahradník, M. Fakis, I. Polyzos, P. Persephonis, *J. Org. Chem.* **2011**, *76*, 8726–8736; b) V. Hrobáriková, P. Hrobárik, P. Gajdoš, I. Fitolis, M. Fakis, P. Persephonis, P. Zahradník, *J. Org. Chem.* **2010**, *75*, 3053–3068; c) Y. M. Poronik, V. Hugues, M. Blanchard-Desce, D. T. Gryko, *Chem. Eur. J.* **2012**, *18*, 9258–9266.
- [11] F. Terenziani, A. Painelli, C. Katan, M. Charlot, M. Blanchard-Desce, *J. Am. Chem. Soc.* **2006**, *128*, 15742–15755.
- [12] a) C. Le Droumaguet, O. Mongin, M. H. V. Werts, M. Blanchard-Desce, *Chem. Commun.* **2005**, 2802–2804; b) C. Katan, F. Terenziani, O. Mongin, M. H. V. Werts, L. Porre's, T. Pons, J. Mertz, S. Tretiak, M. Blanchard-Desce, *J. Phys. Chem. A* **2005**, *109*, 3024–3037; c) S. Amthor, C. Lambert, S. Dümmler, I. Fischer, J. Schelter, *J. Phys. Chem. A* **2006**, *110*, 5204–5214; d) W. Kim, J. Sung, M. Grzybowski, D. T. Gryko, D. Kim, *J. Phys. Chem. Lett.* **2016**, *7*, 3060–3066; e) B. Dereka, A. Rosspeintner, M. Krzeszewski, D. T. Gryko, E. Vauthey, *Angew. Chem. Int. Ed.* **2016**, *55*, 15624–15628; *Angew. Chem.* **2016**, *128*, 15853–15857.
- [13] a) A. Janiga, D. T. Gryko, *Chem. Asian J.* **2014**, *9*, 3036–3045; b) M. Krzeszewski, T. Kodama, E. M. Espinoza, V. I. Vullev, T. Kubo, D. T. Gryko, *Chem. Eur. J.* **2016**, *22*, 16478–16488; c) A. Janiga, M. Krzeszewski, D. T. Gryko, *Chem. Asian J.* **2015**, *10*, 212–218; d) M. Tasiar, M. Chotkowski, D. T. Gryko, *Org. Lett.* **2015**, *17*, 6106–6109; e) R. Stężycki, M. Grzybowski, G. Clermont, M. Blanchard-Desce, D. T. Gryko, *Chem. Eur. J.* **2016**, *22*, 5198–5203.
- [14] D. H. Friese, A. Mikhaylov, M. Krzeszewski, Y. M. Poronik, A. Rebane, K. Ruud, D. T. Gryko, *Chem. Eur. J.* **2015**, *21*, 18364–18374.
- [15] a) M. Barzoukas, M. Blanchard-Desce, *J. Chem. Phys.* **2000**, *113*, 3951–3959; b) M. Drobizhev, A. Karotki, Y. Dzenis, A. Rebane, Z. Suo, C. W. Spangler, *J. Phys. Chem. B* **2003**, *107*, 7540–7543; c) H. Meier, *Angew. Chem. Int. Ed.* **2005**, *44*, 2482–2506; *Angew. Chem.* **2005**, *117*, 2536–2561; d) M. Charlot, N. Izard, O. Mongin, D. Riehl, M. Blanchard-Desce, *Chem. Phys. Lett.* **2006**, *417*, 297–302; e) Y. Niko, H. Morimoto, H. Sugihara, Y. Suzuki, J. Kawamata, G.-I. Konishi, *J. Mater. Chem. B* **2015**, *3*, 184–190.
- [16] a) M. Dal Molin, Q. Verolet, S. Soleimanpour, S. Matile, *Chem. Eur. J.* **2015**, *21*, 6012–6021; b) H. M. Kim, W. J. Yang, C. H. Kim, W.-H. Park, S.-J. Jeon, B. R. Cho, *Chem. Eur. J.* **2005**, *11*, 6386–6391; c) M. Murai, S.-Y. Ku, N. D. Treat, M. J. Robb, M. L. Chabincyn, C. J. Hawker, *Chem. Sci.* **2014**, *5*, 3753–3760.
- [17] A. Janiga, E. Glodkowska-Mrowka, T. Stoklosa, D. T. Gryko, *Asian J. Org. Chem.* **2013**, *2*, 411–415.
- [18] A. Janiga, D. Bednarska, B. Thorsted, J. Brewer, D. T. Gryko, *Org. Biomol. Chem.* **2014**, *12*, 2874–2881.
- [19] M. Krzeszewski, B. Thorsted, J. Brewer, D. T. Gryko, *J. Org. Chem.* **2014**, *79*, 3119–3128.
- [20] R. Orłowski, M. Banasiewicz, G. Clermont, F. Castet, R. Nazir, M. Blanchard-Desce, D. T. Gryko, *Phys. Chem. Chem. Phys.* **2015**, *17*, 23724–23731.
- [21] D. S. Surry, S. L. Buchwald, *Chem. Sci.* **2011**, *2*, 27–50.
- [22] F. W. Goldberg, J. G. Kettle, J. Xiong, D. Lin, *Tetrahedron* **2014**, *70*, 6613–6622.
- [23] a) M. Krzeszewski, D. T. Gryko, *J. Org. Chem.* **2015**, *80*, 2893–2899; b) A. Pradhan, P. Dechambenoit, H. Bock, F. Durola, *Chem. Eur. J.* **2016**, *22*, 18227–18235.
- [24] a) F. Bellina, R. Rossi, *Adv. Synth. Catal.* **2010**, *352*, 1223–1276; b) D. Alberico, M. E. Scott, M. Lautens, *Chem. Rev.* **2007**, *107*, 174–238; c) J. Pschierer, H. Plenio, *Angew. Chem. Int. Ed.* **2010**, *49*, 6224–6227; *Angew. Chem.* **2010**, *122*, 6361–6364; d) D. T. Gryko, O. Vakuliuk, D. Gryko, B. Koszarna, *J. Org. Chem.* **2009**, *74*, 9517–9520; e) D. Liégault, L. Lapointe, A. Caron, A. Vlassova, K. Fagnou, *J. Org. Chem.* **2009**, *74*, 1826–1834; f) P. Ehlers, A. Petrosyan, J. Baumgard, S. Jopp, N. Steinfeld, T. Ghochikyan, V. Saghyan, C. Fischer, P. Langer, *ChemCatChem* **2013**, *5*, 2504–2511.
- [25] a) Y. Xu, L. Zhao, Y. Li, H. Doucet, *Adv. Synth. Catal.* **2013**, *355*, 1423–1432; b) L. Zhao, C. Bruneau, H. Doucet, *ChemCatChem* **2013**, *5*, 255–262.
- [26] A. Rebane, G. Wicks, M. Drobizhev, T. Cooper, A. Trummal, M. Uudsemaa, *Angew. Chem. Int. Ed.* **2015**, *54*, 7582–7586; *Angew. Chem.* **2015**, *127*, 7692–7696.
- [27] A. Rebane, N. S. Makarov, M. Drobizhev, B. Spangler, E. S. Tarter, B. D. Reeves, C. W. Spangler, F. Meng, Z. Suo, *J. Phys. Chem. C* **2008**, *112*, 7997–8004.
- [28] A. Mikhaylov, E. Arias, I. Moggio, R. Ziolo, M. Uudsemaa, A. Trummal, T. Cooper, A. Rebane, *Proc. SPIE* **2017**, 10101,1010117.
- [29] M. Drobizhev, N. S. Makarov, S. E. Tillo, T. E. Hughes, A. Rebane, *J. Phys. Chem. B* **2012**, *116*, 1736–1744.
- [30] A. Nowak-Król, C. J. Wilson, M. Drobizhev, D. V. Kondratuk, A. Rebane, H. L. Anderson, D. T. Gryko, *ChemPhysChem* **2013**, *13*, 3966–3972.
- [31] B. Dereka, A. Rosspeintner, Z. Li, R. Liska, E. Vauthey, *J. Am. Chem. Soc.* **2016**, *138*, 4643–4649.
- [32] S. de Reguardati, J. Pahapill, A. Mikhailov, Y. Stepanenko, A. Rebane, *Opt. Express* **2016**, *24*, 9053–9066.
- [33] A. Rebane, M. Drobizhev, N. S. Makarov, G. Wicks, P. Wnuk, Y. Stepanenko, J. E. Haley, D. M. Krein, J. L. Fore, A. R. Burke, J. E. Slagle, D. G. McLean, T. M. Cooper, *J. Phys. Chem. A* **2014**, *118*, 3749–3759.
- [34] F. Santoro, B. Le Guennic, *Wires Comput. Mol. Sci.* **2016**, *6*, 460–486.
- [35] N. S. Makarov, M. Drobizhev, A. Rebane, *Opt. Express* **2008**, *16*, 4029–4047.

- [36] G. G. Dubinina, R. S. Price, K. A. Abboud, G. Wicks, P. Wnuk, Y. Stepanenko, M. Drobizhev, A. Rebane, K. S. Schanze, *J. Am. Chem. Soc.* **2012**, *134*, 19346–19349.
- [37] Gaussian 09 Revision D.01, M. J. Frisch, G. W. Trucks, H. B. Schlegel, G. E. Scuseria, M. A. Robb, J. R. Cheeseman, G. Scalmani, V. Barone, B. Mennucci, G. A. Petersson, H. Nakatsuji, M. Caricato, X. Li, H. P. Hratchian, A. F. Izmaylov, J. Bloino, G. Zheng, J. L. Sonnenberg, M. Hada, M. Ehara, K. Toyota, R. Fukuda, J. Hasegawa, M. Ishida, T. Nakajima, Y. Honda, O. Kitao, H. Nakai, T. Vreven, J. A. Montgomery, Jr., J. E. Peralta, F. Ogliaro, M. Bearpark, J. J. Heyd, E. Brothers, K. N. Kudin, V. N. Staroverov, R. Kobayashi, J. Normand, K. Raghavachari, A. Rendell, J. C. Burant, S. S. Iyengar, J. Tomasi, M. Cossi, N. Rega, J. M. Millam, M. Klene, J. E. Knox, J. B. Cross, V. Bakken, C. Adamo, J. Jaramillo, R. Gomperts, R. E. Stratmann, O. Yazyev, A. J. Austin, R. Cammi, C. Pomelli, J. W. Ochterski, R. L. Martin, K. Morokuma, V. G. Zakrzewski, G. A. Voth, P. Salvador, J. J. Dannenberg, S. Dapprich, A. D. Daniels, O. Farkas, J. B. Foresman, J. V. Ortiz, J. Cioslowski, D. J. Fox, Gaussian Inc. Wallingford CT, **2009**.
- [38] K. Aidas, C. Angeli, K. L. Bak, V. Bakken, R. Bast, L. Boman, O. Christiansen, R. Cimiraglia, S. Coriani, P. Dahle, E. K. Dalskov, U. Ekström, T. Enevoldsen, J. J. Eriksen, P. Ettenhuber, B. Fernández, L. Ferrighi, H. Fliegl, L. Frediani, K. Hald, A. Halkier, C. Hättig, H. Heiberg, T. Helgaker, A. C. Hennum, H. Hettema, E. Hjertenæs, S. Høst, I.-M. Høyvik, M. F. Iozzi, B. Jansik, H. J. Aa. Jensen, D. Jonsson, P. Jørgensen, J. Kauczor, S. Kirpekar, T. Kjærgaard, W. Klopper, S. Knecht, R. Kobayashi, H. Koch, J. Kongsted, A. Krapp, K. Kristensen, A. Ligabue, O. B. Lutnæs, J. I. Melo, K. V. Mikkelsen, R. H. Myhre, C. Neiss, C. B. Nielsen, P. Norman, J. Olsen, J. M. H. Olsen, A. Osted, M. J. Packer, F. Pawłowski, T. B. Pedersen, P. F. Provasi, S. Reine, Z. Rinkevicius, T. A. Ruden, K. Ruud, V. Rybkin, P. Salek, C. C. M. Samson, A. Sánchez de Merás, T. Saue, S. P. A. Sauer, B. Schimmelpfennig, K. Sneskov, A. H. Steindal, K. O. Sylvester-Hvid, P. R. Taylor, A. M. Teale, E. I. Tellgren, D. P. Tew, A. J. Thorvaldsen, L. Thøgersen, O. Vahtras, M. A. Watson, D. J. D. Wilson, M. Ziolkowski, H. Ågren, *WIREs Comput. Mol. Sci.* **2014**, *4*, 269–284.
- [39] Y. Zhao, D. G. Truhlar, *Theor. Chem. Acc.* **2008**, *120*, 215–241.
- [40] B. Le Guennic, D. Jacquemin, *Acc. Chem. Res.* **2015**, *48*, 530–537.
- [41] J. Tomasi, B. Mennucci, R. Cammi, *Chem. Rev.* **2005**, *105*, 2999–3094.
- [42] M. Caricato, B. Mennucci, J. Tomasi, F. Ingrosso, R. Cammi, S. Corni, G. Scalmani, *J. Chem. Phys.* **2006**, *124*, 124520.
- [43] F. Santoro, FCclasses, a Fortran 77 Code, **2011**, code available at: <http://village/pi.iccom.cnr.it>.
- [44] F. Santoro, R. Improta, A. Lami, J. Bloino, V. Barone, *J. Chem. Phys.* **2007**, *126*, 084509.
- [45] T. Yanai, D. P. Tew, C. Handy, *Chem. Phys. Lett.* **2004**, *393*, 51–57.

---

Manuscript received: February 1, 2017  
 Revised manuscript received: April 10, 2017  
 Accepted manuscript online: April 11, 2017  
 Version of record online: June 8, 2017